Supplement of Hydrol. Earth Syst. Sci., 28, 4577–4597, 2024
https://doi.org/10.5194/hess-28-4577-2024-supplement

Hydrology and Earth System Sciences
Open Access
EGU

Supplement of

Catchment response to climatic variability: implications for root zone storage and streamflow predictions

Nienke Tempel et al.

Correspondence to: Nienke Tempel (nienketessatempel@gmail.com)

S1. Budyko plot per decade

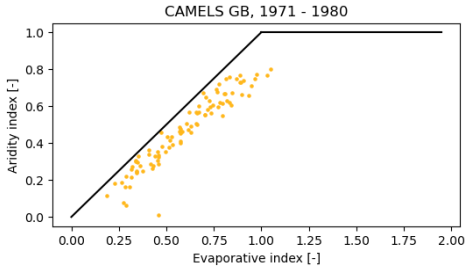

(a)

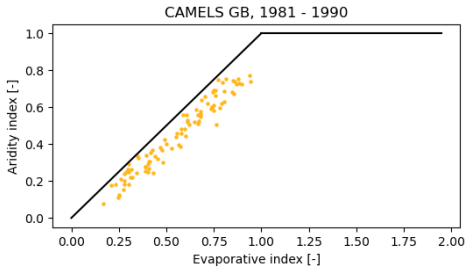

(b)

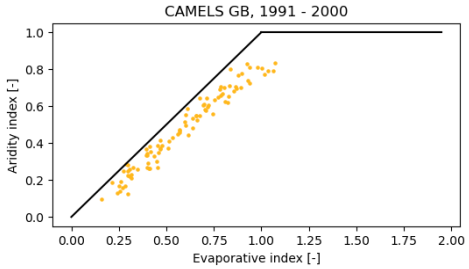

(c)

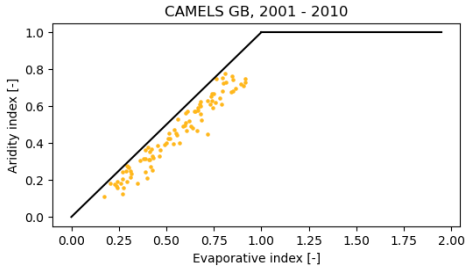

(d)

Figure S1: Budyko plot (illustration of the long-term average values) per decade for CAMELS GB: (a) 1971 - 1980, (b) 1981 - 1990, (c) 1991 - 2000, (d) 2001 - 2010.

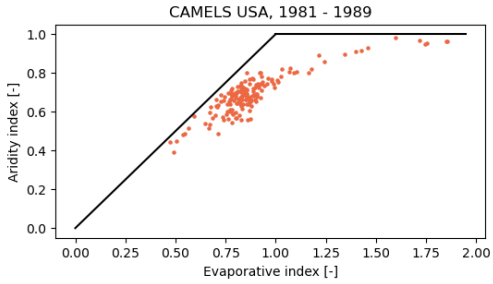

(a)

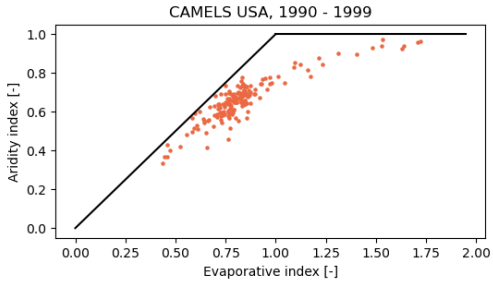

(b)

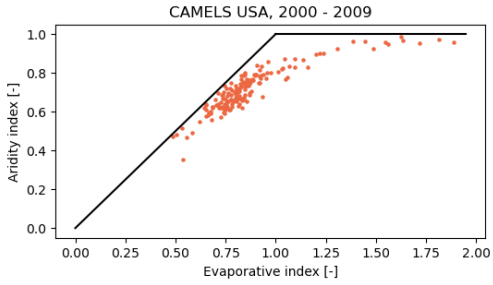

(c)

Figure S2: Budyko plot (illustration of the long-term average values) per decade for CAMELS USA: (a) 1981 - 1989, (b) 1990 - 1999, (c) 2000 - 2009.

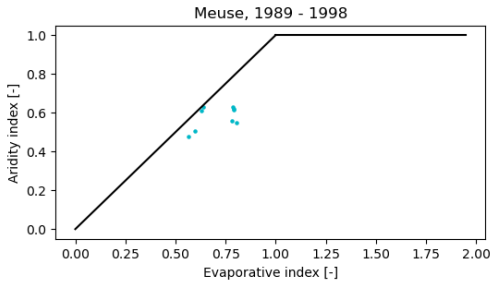

(a)

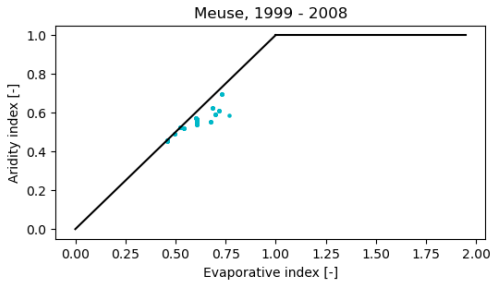

(b)

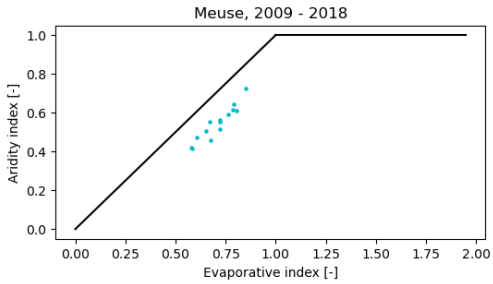

(c)

Figure S3: Budyko plot (illustration of the long-term average values) per decade for Meuse: (a) 1989 - 1998, (b) 1999 - 2008, (c) 2009 - 2018. Note that the first decade has fewer data points due to limited data availability.

S2. Geographical plots of ΔI_E

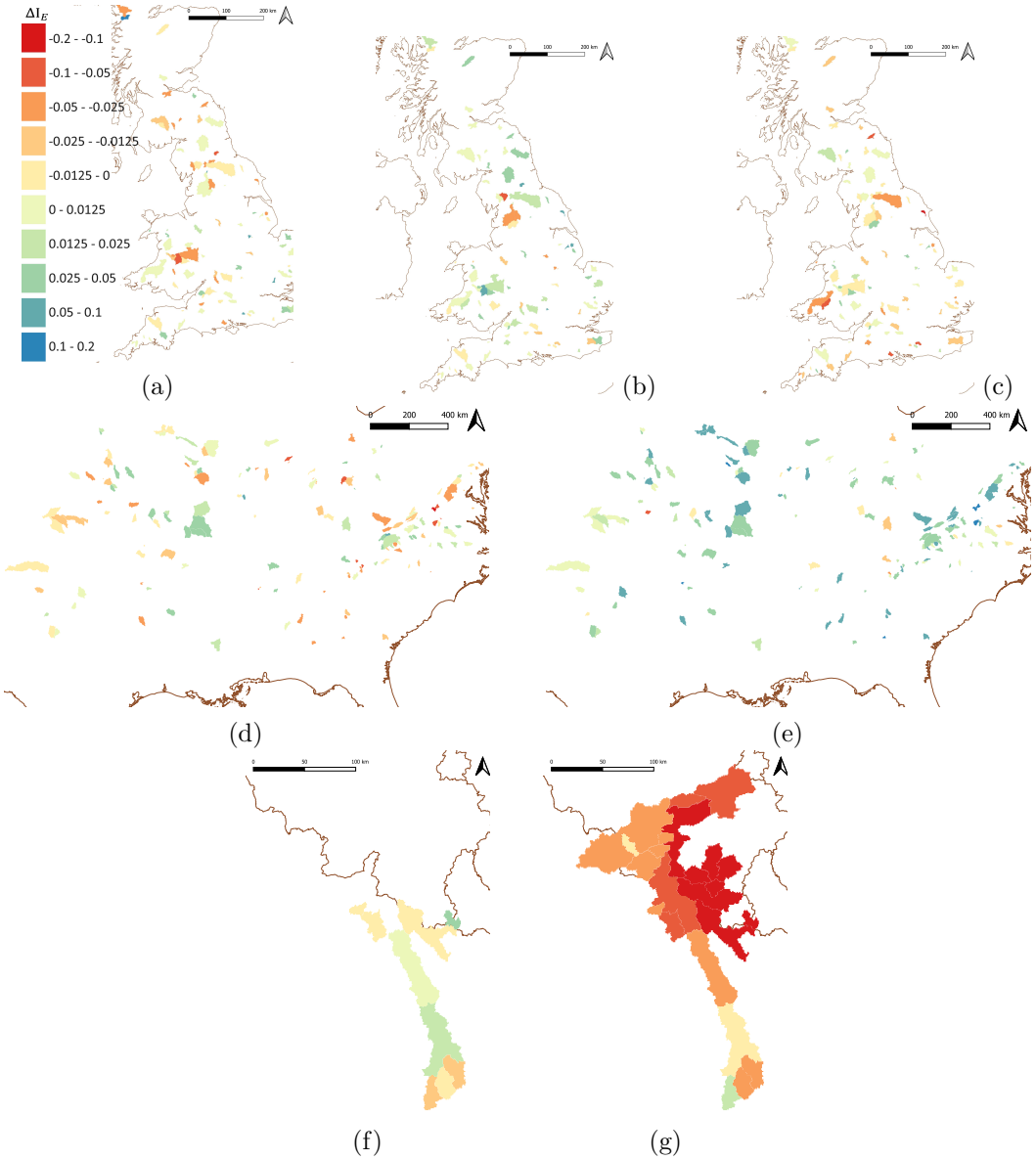

Figure S4: Errors in estimating I_E for different time periods across multiple regions. The first row represents the GB region for the periods (a) 1981-1990, (b) 1991-2000, and (c) 2001 - 2010. The second row represents the USA region for the periods (d) 1990-1999 and (e) 2000-2009. The third row represents the Meuse region for the periods (f) 1999-2008 and (g) 2009-2018. In all figures, the colours indicate the error in I_E (ΔI_E), ranging from -0.2 (red) to +0.2 (blue).

S3. Scenarios A-2 and B-2

Distinctions are also made based on which period is used to make a prediction about the other period (1 or 2). Scenario 1 (A/B) is generated by utilising the omega value of the first decade (p1, 1999-2008) to predict the root zone storage capacity for the second decade (p2, 2009-2018). The model is then executed for the period of 2009-2018. Scenario 2 (A-2/B-2) makes predictions by reversing time. The omega value of the second decade (p2, 2009-2018) is used to predict the root zone storage capacity for the first decade (p1, 1999-2008), meaning that the model is executed for the period of the first decade (p1, 1999-2008).

- *Scenario A* uses the omega value of p1 with a sampled ΔI_E from the distribution calculated from all the data (Meuse, CAMELS USA, CAMELS GB) to make a prediction about the evaporation and root zone storage capacity of p2, 2009-2018.
- *Scenario A-2* uses the omega value of p1 with a sampled ΔI_E from the distribution calculated from all the data (Meuse, CAMELS USA, CAMELS GB) to make a prediction about the evaporation and root zone storage capacity of p1, 1999-2008.
- *Scenario B* uses the omega value of p1 with a sampled ΔI_E from the distribution calculated from the Meuse data to make a prediction about the evaporation and root zone storage capacity of p2, 2009-2018.
- *Scenario B-2* uses the omega value of p1 with a sampled ΔI_E from the distribution calculated from the Meuse data to make a prediction about the evaporation and root zone storage capacity of p1, 1999-2008.

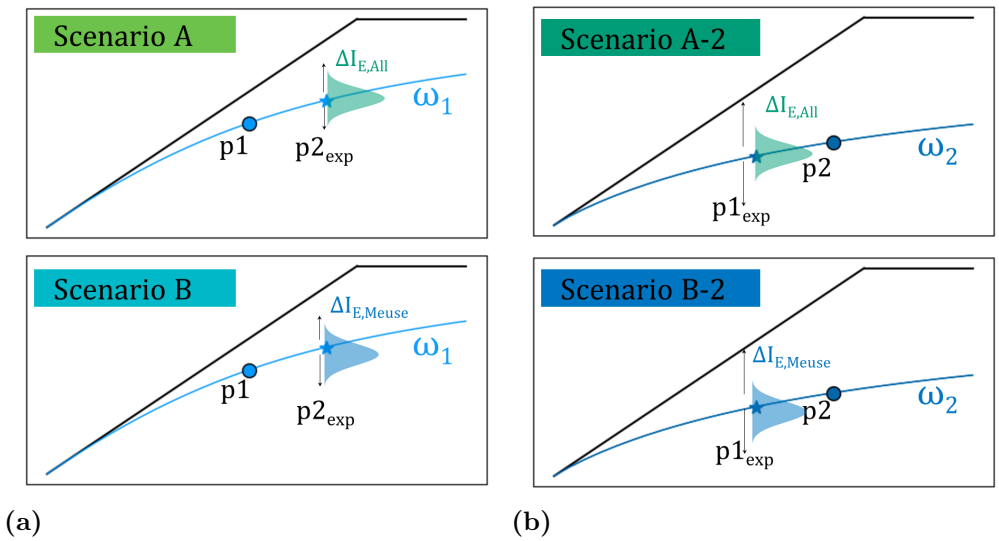

Figure S5: Overview of the scenario structures. p1 is the time period of 1999-2008 and p2 of 2009-2018. (a) Scenario structure variant 1 (b) Scenario structure variant 2

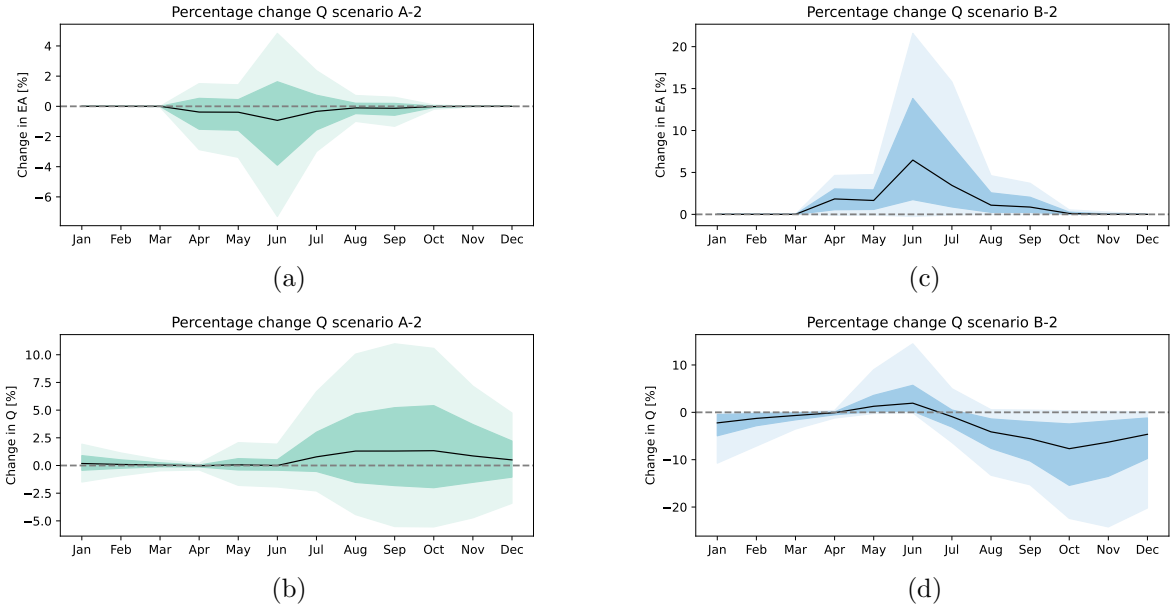

Figure S6: Change in evaporation and streamflow for scenarios A-2 and B-2. The change is calculated for every run as the difference between the evaporation or streamflow with the reference run ($\Delta I_E = 0$). The output for all years, catchments, and runs has been put together. The lightly shaded area represents the 90th and 10th percentiles, while the slightly darker shaded area represents the 25th to 75th percentiles. The black line represents the median.

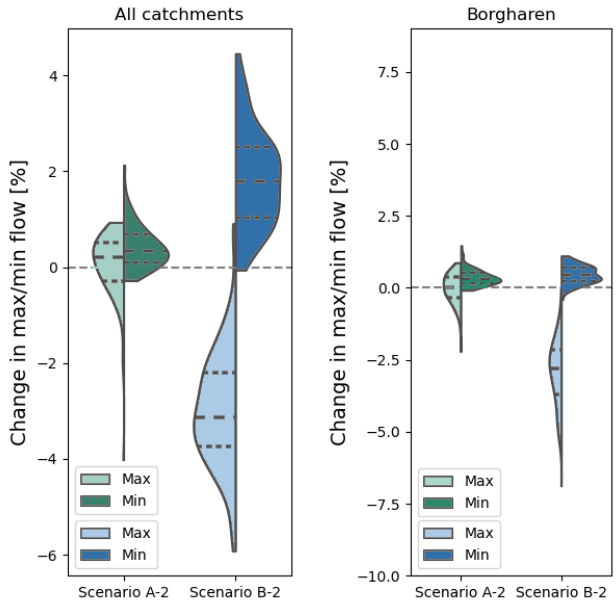

Figure S7: Change in maximum flow ($Q_{\max}$, left part of the violin) and 7-day minimum flow ($Q_{\min}$, right part of the violin), in percentage of the reference run, for (a) all catchments together and (b) Borharen. The quartiles are indicated with dashed lines.

S4. Variability of ΔI_E and ΔI_A across catchments

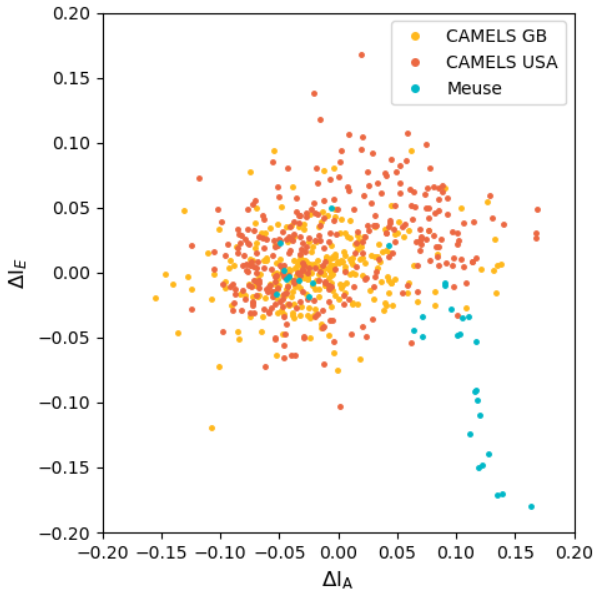

Figure S8: Scatter plot illustrating the relationship between the deviations of ΔI_A and ΔI_E across different catchments. Data points represent catchments from CAMELS GB, CAMELS USA, and Meuse datasets in different time periods.

S5. Performance measurement of wflow-Flextopo

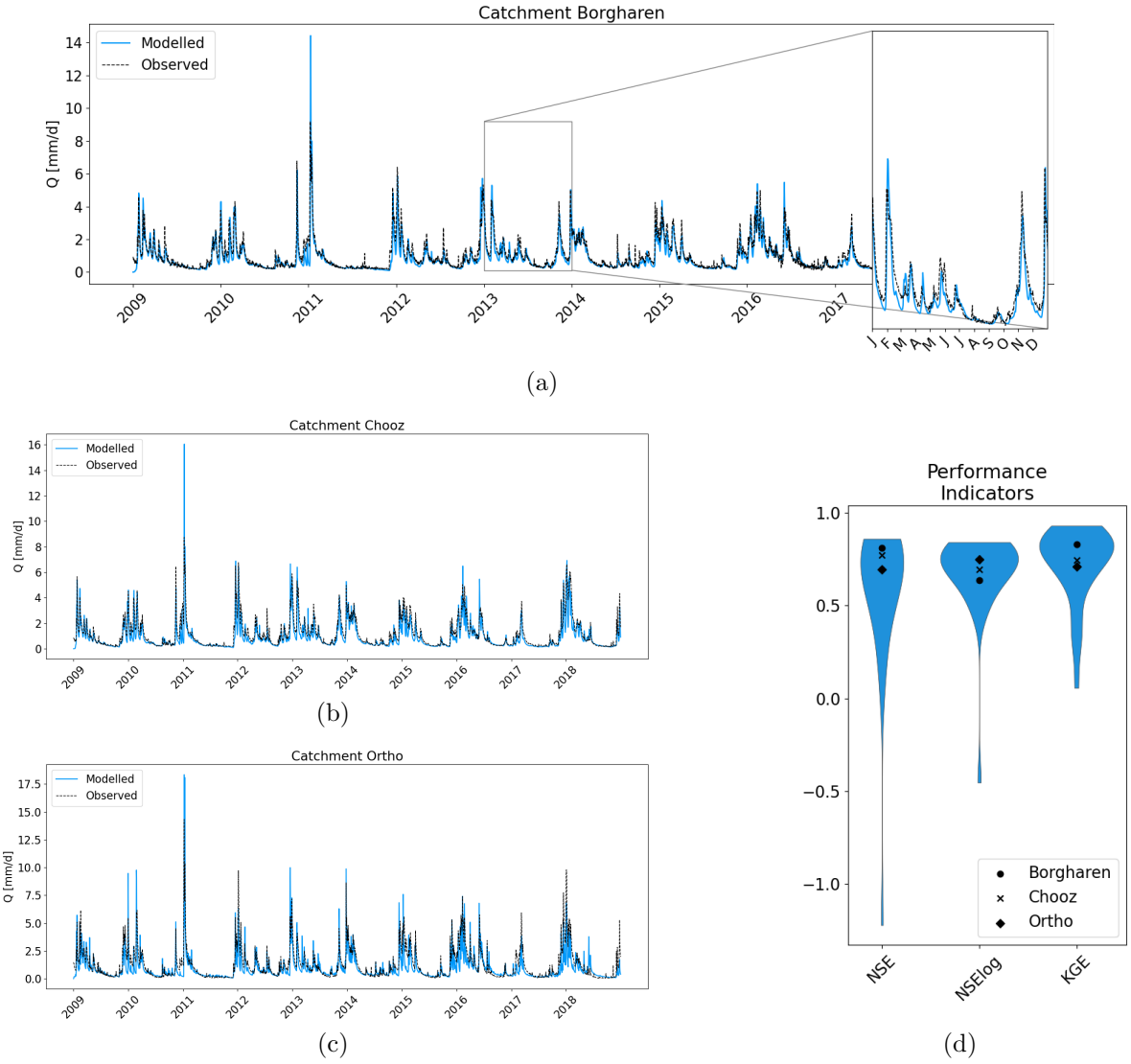

Figure S9: Performance measurement through (a) hydrograph of modeled and observed streamflow in catchment Borgharen, (b) Ortho, (c) Chooz and (d) performance indicators calculated for the time period of each scenario: Nash-Sutcliffe efficiencies of streamflow (NSE), the logarithm of streamflow (NSElog), and Kling-Gupta efficiency of streamflow (KGE). The bandwidth of each violin represents the distribution of performance across different catchments and the catchments from (a), (b) and (c) are indicated.

S6. Change in flow per catchment

The following images show the outcomes of the model concerning alterations in evaporation and streamflow for each catchment. The changes in evaporation (EA) and streamflow (Q) are represented in units of [mm/d]. To calculate the change, the difference between evaporation or streamflow and the reference run ($\Delta I_E = 0$) was determined for each run. The results for all years and runs were then aggregated. The 90th and 10th percentiles are depicted in the lightly shaded area, while the slightly darker shaded area represents the 25th to 75th percentiles. The median is denoted by the black line.

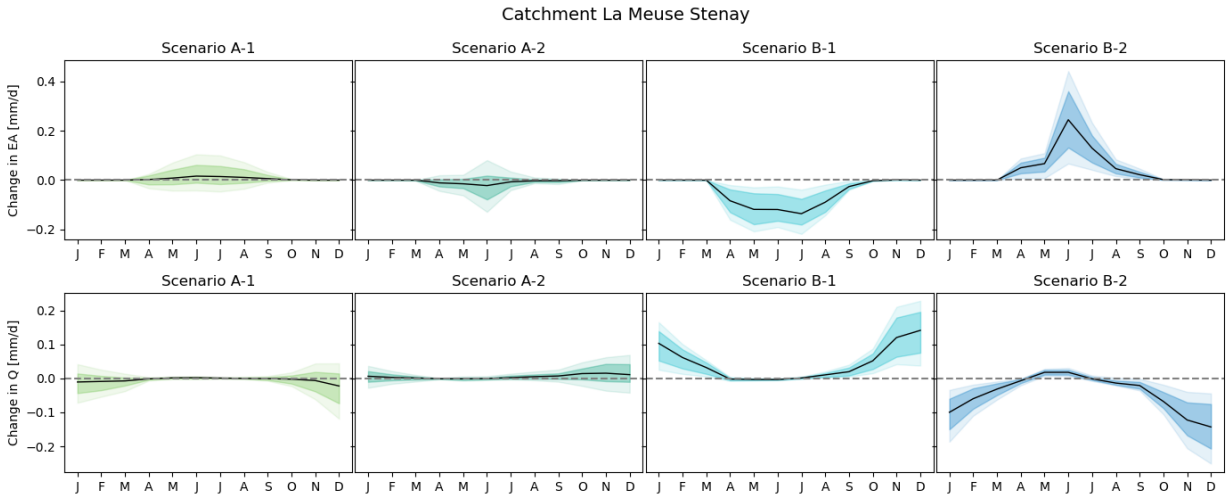

Figure S10: Change in evaporation (EA) and streamflow (Q), both in [mm/d] for La Meuse Stenay.

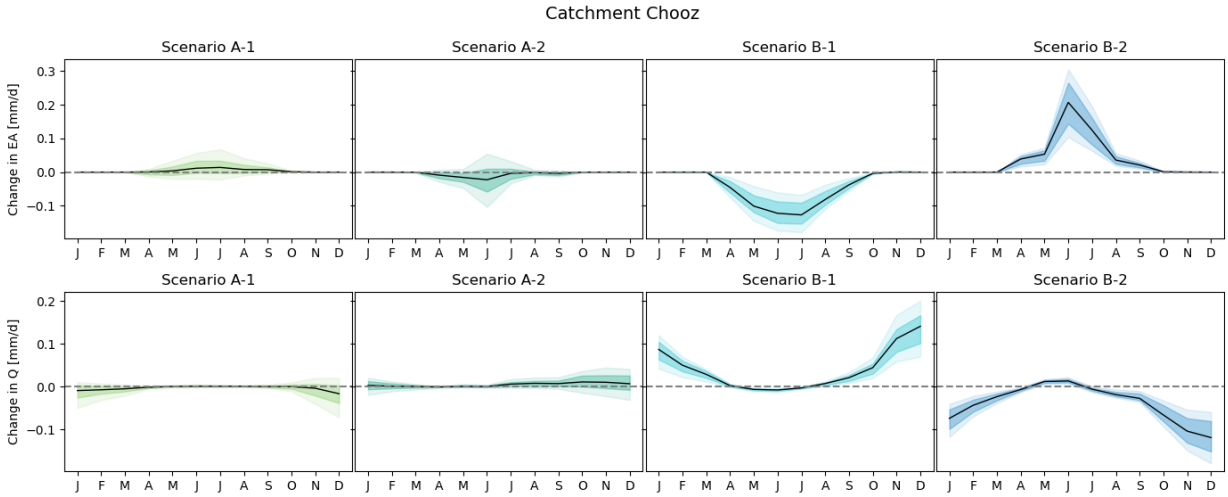

Figure S11: Change in evaporation (EA) and streamflow (Q), both in [mm/d] for Chooz.

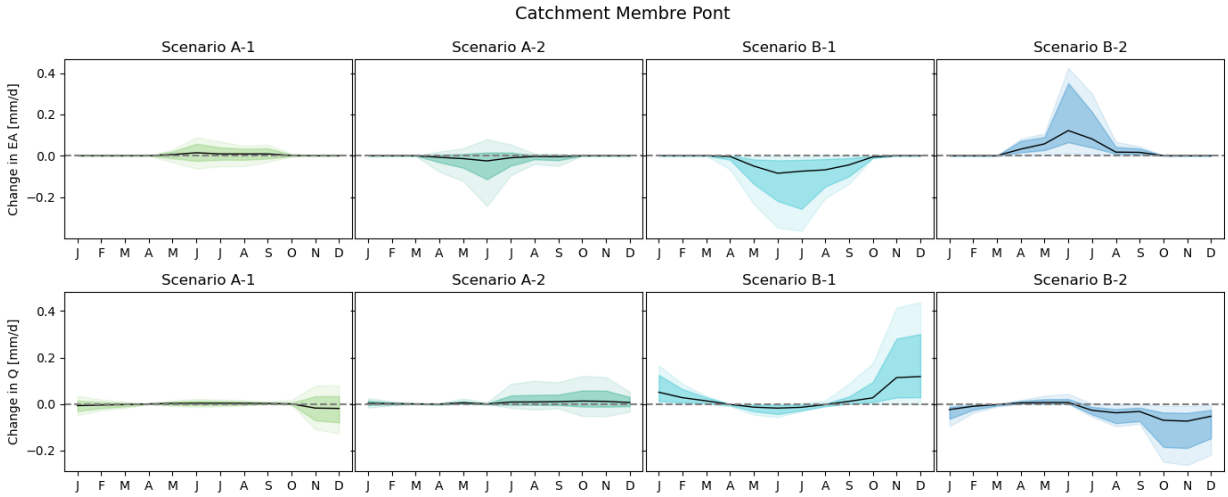

Figure S12: Change in evaporation (EA) and streamflow (Q), both in [mm/d] for Membre Pont.

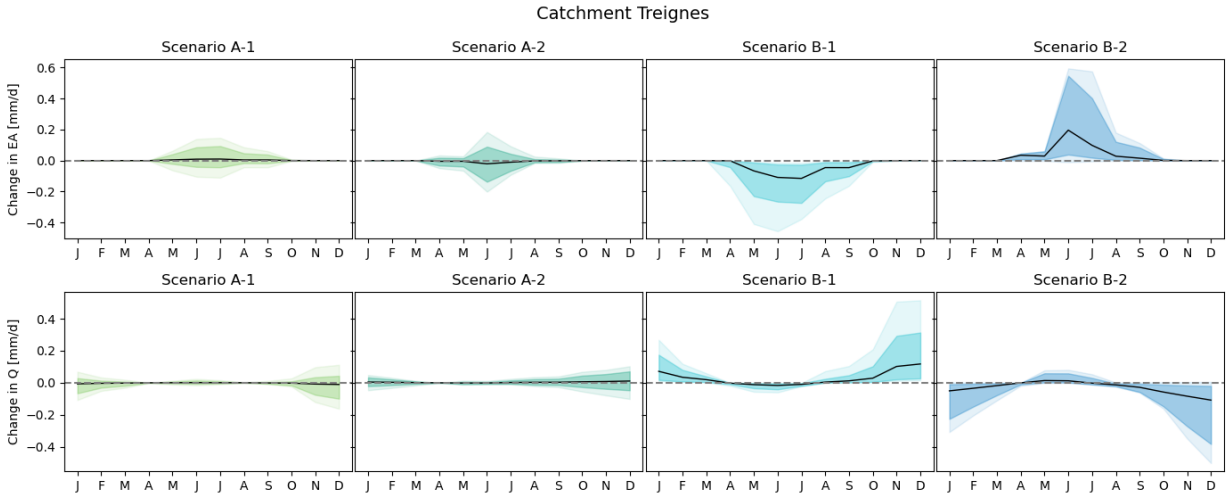

Figure S13: Change in evaporation (EA) and streamflow (Q), both in [mm/d] for Treignes.

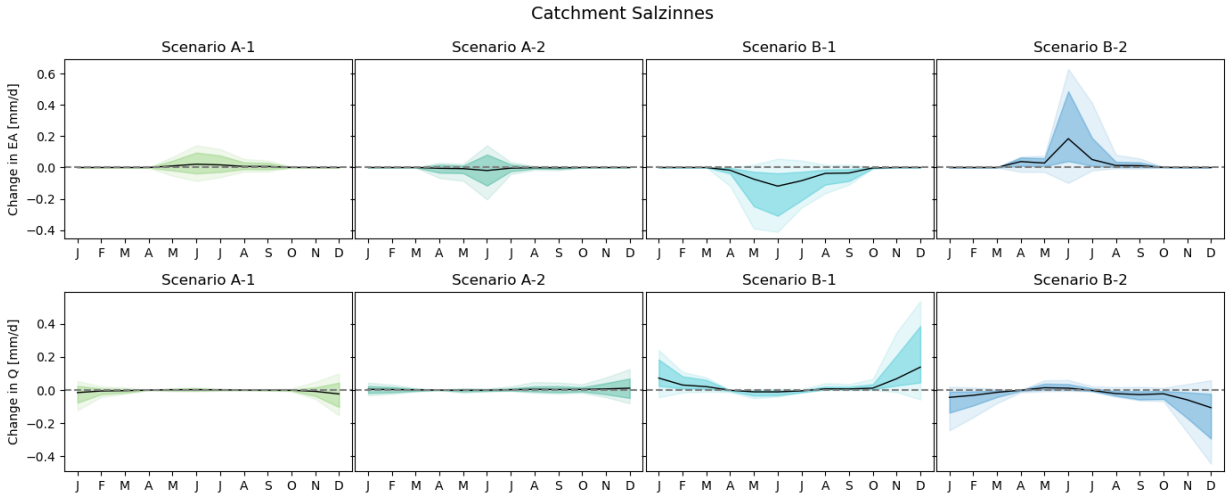

Figure S14: Change in evaporation (EA) and streamflow (Q), both in [mm/d] for Salzinnes.

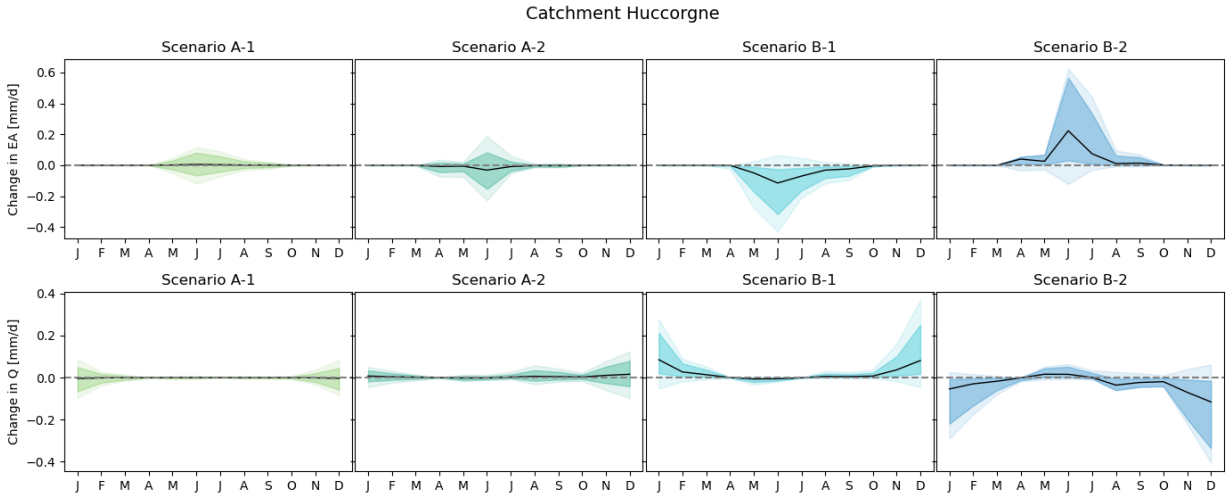

Figure S15: Change in evaporation (EA) and streamflow (Q), both in [mm/d] for Huccorgne.

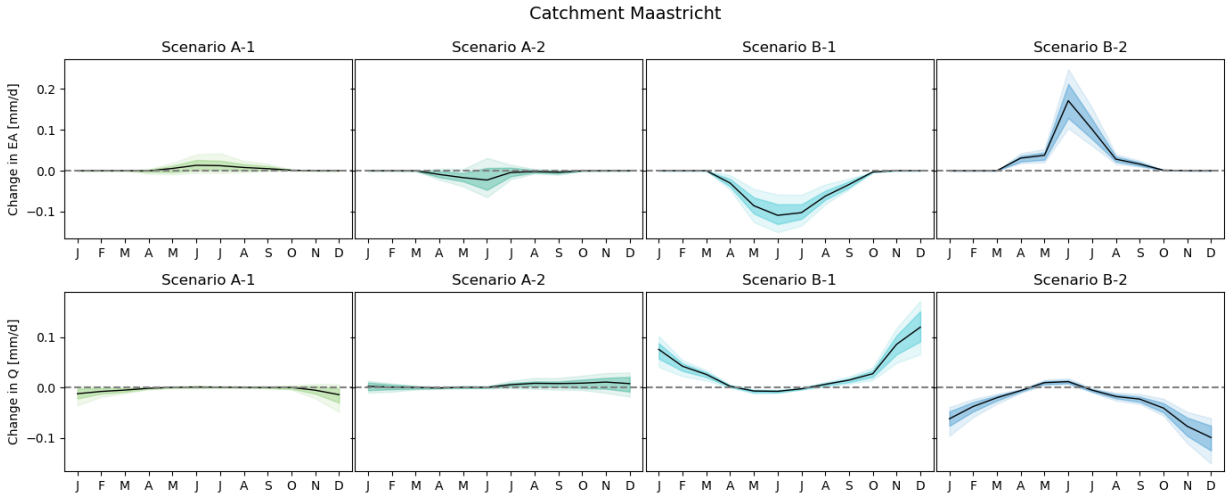

Figure S16: Change in evaporation (EA) and streamflow (Q), both in [mm/d] for Borgharen.

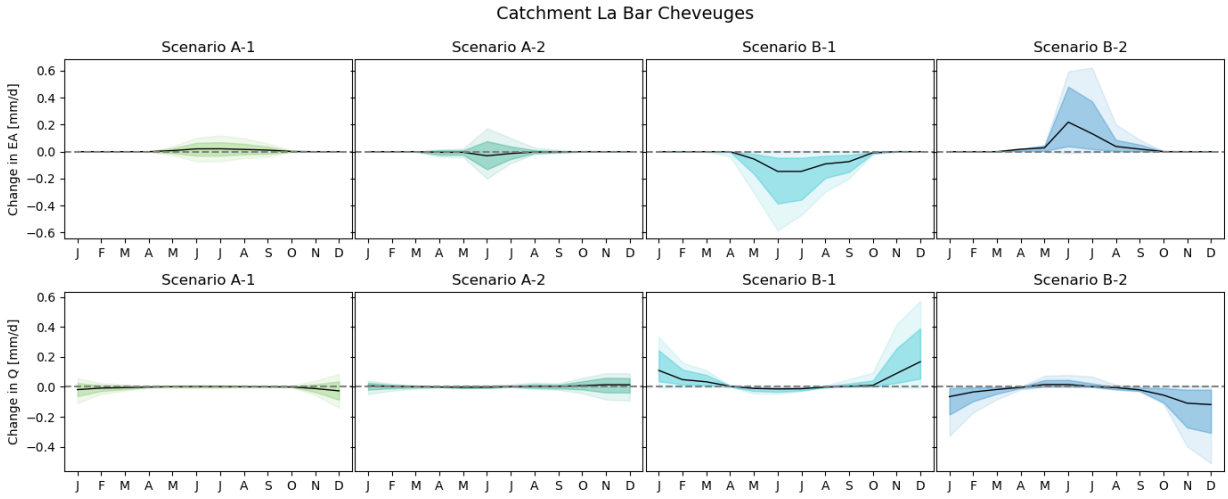

Figure S17: Change in evaporation (EA) and streamflow (Q), both in [mm/d] for La Bar Cheveuges.

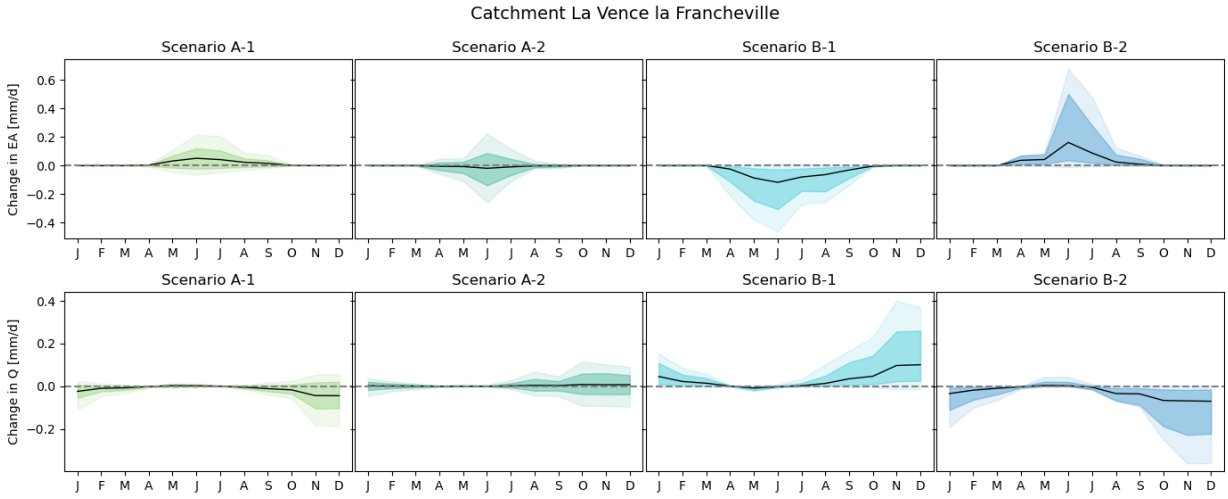

Figure S18: Change in evaporation (EA) and streamflow (Q), both in [mm/d] for La Vence la Francheville.

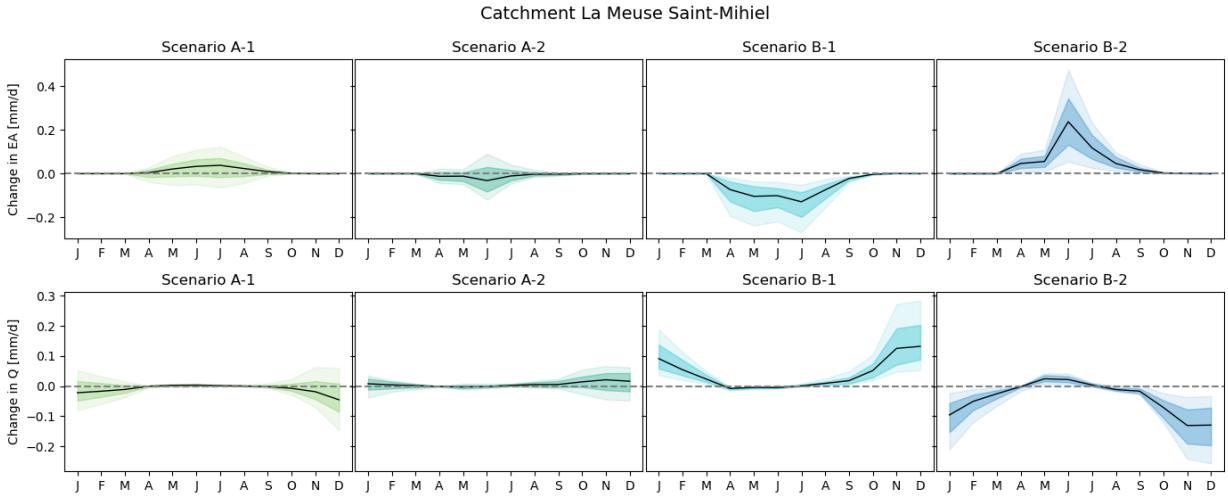

Figure S19: Change in evaporation (EA) and streamflow (Q), both in [mm/d] for La Meuse Saint Mihiel.

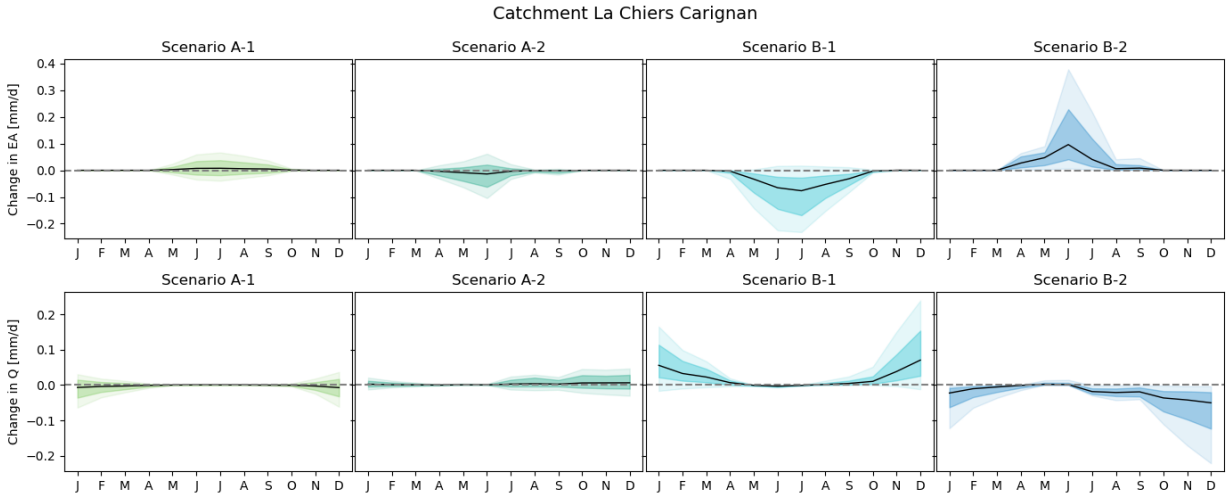

Figure S20: Change in evaporation (EA) and streamflow (Q), both in [mm/d] for La Chiers Carignan.

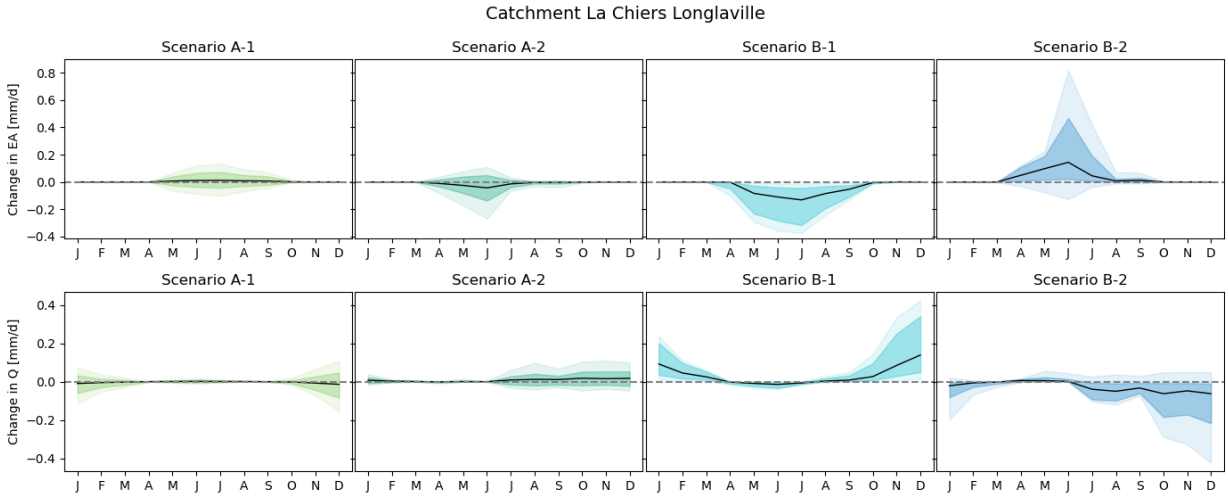

Figure S21: Change in evaporation (EA) and streamflow (Q), both in [mm/d] for La Chiers Longlaville.

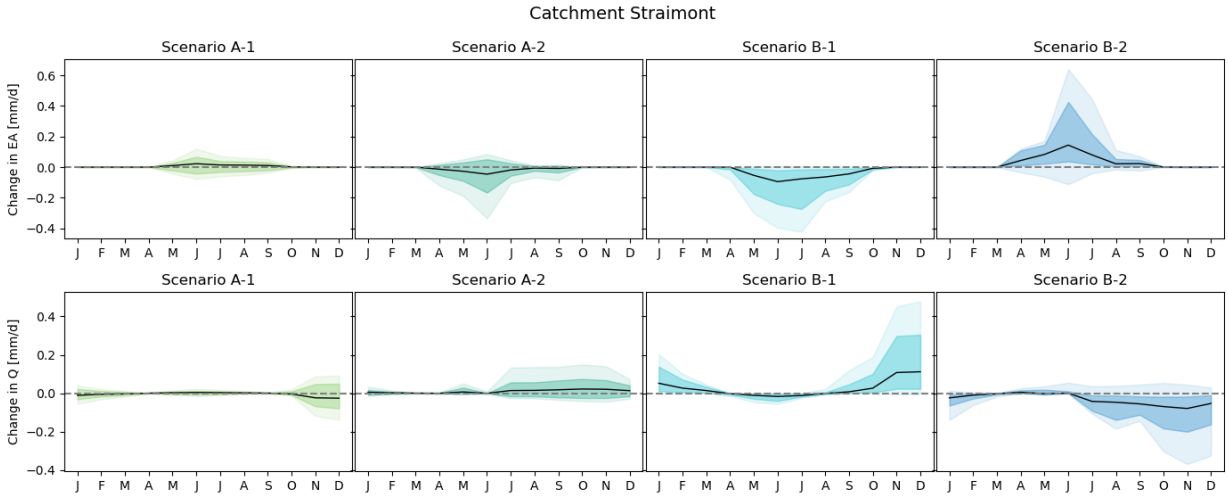

Figure S22: Change in evaporation (EA) and streamflow (Q), both in [mm/d] for Staimont.

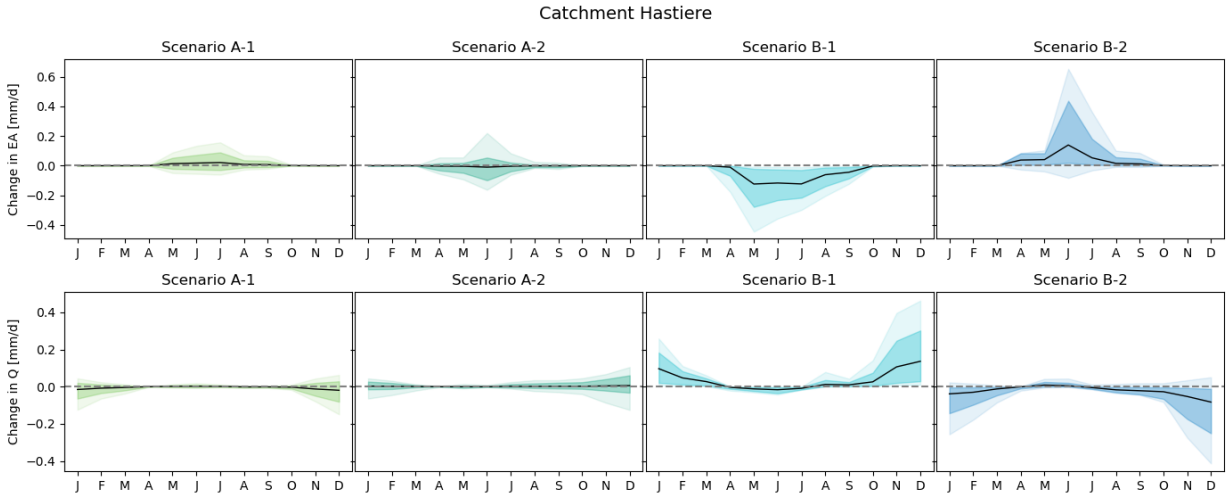

Figure S23: Change in evaporation (EA) and streamflow (Q), both in [mm/d] for Hastiere.

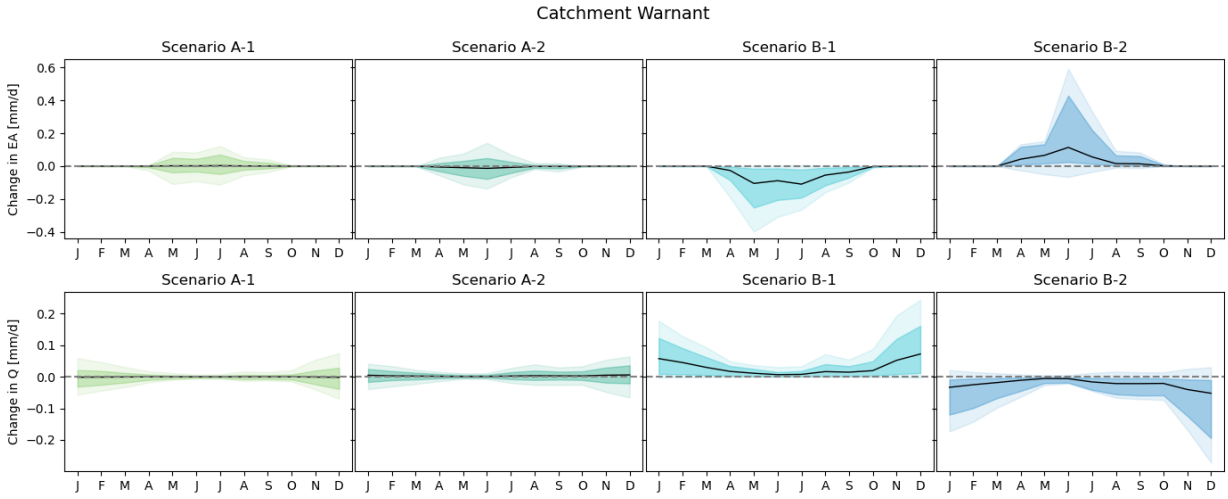

Figure S24: Change in evaporation (EA) and streamflow (Q), both in [mm/d] for Warnant.

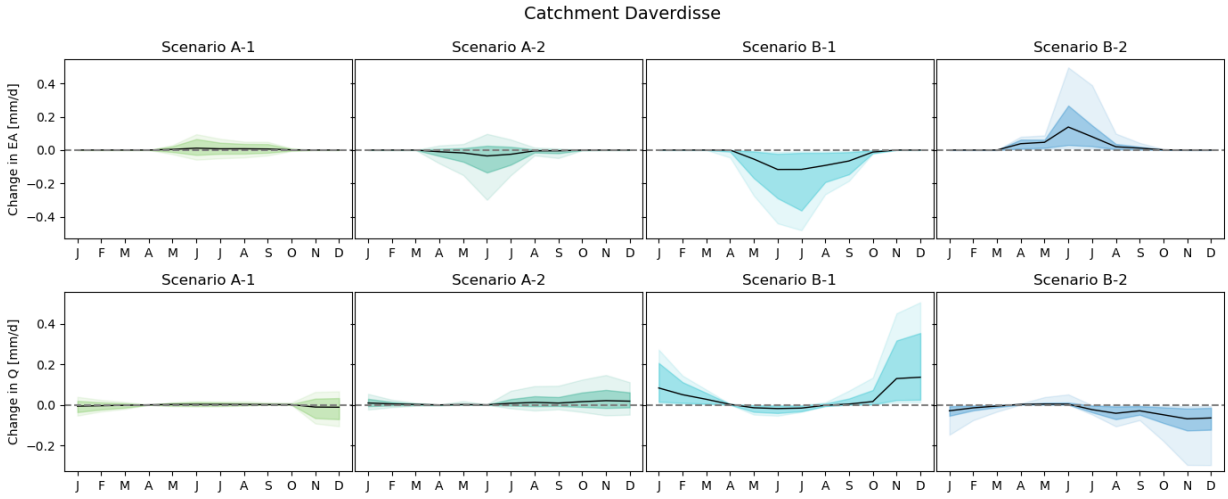

Figure S25: Change in evaporation (EA) and streamflow (Q), both in [mm/d] for Daverdisse.

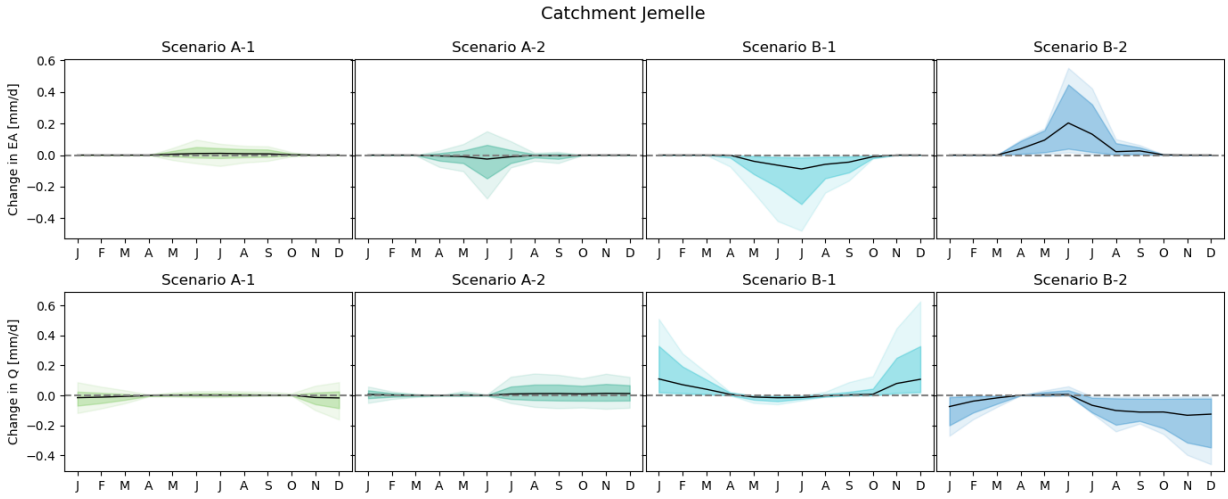

Figure S26: Change in evaporation (EA) and streamflow (Q), both in [mm/d] for Jemelle.

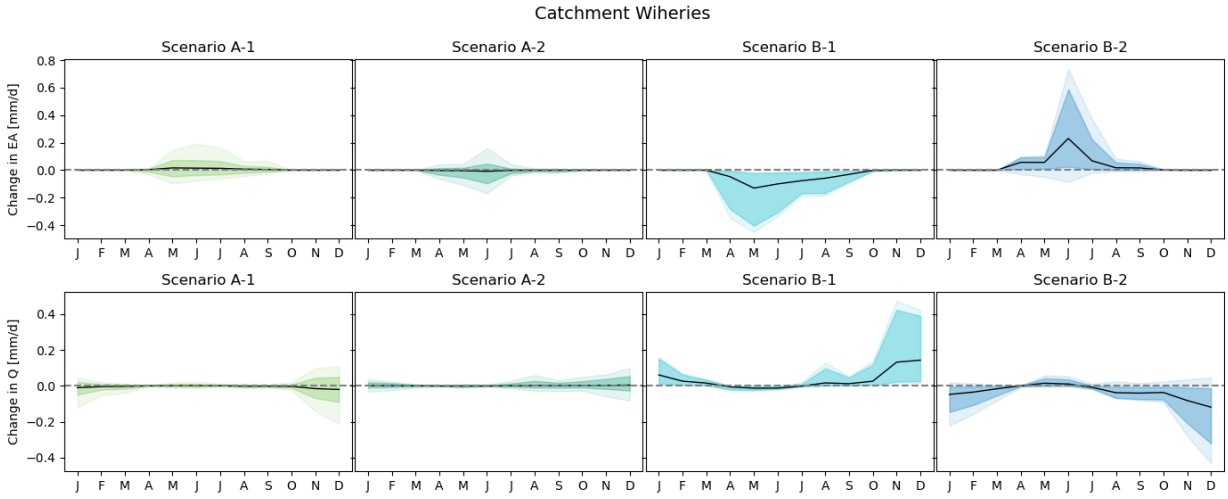

Figure S27: Change in evaporation (EA) and streamflow (Q), both in [mm/d] for Wiheries.

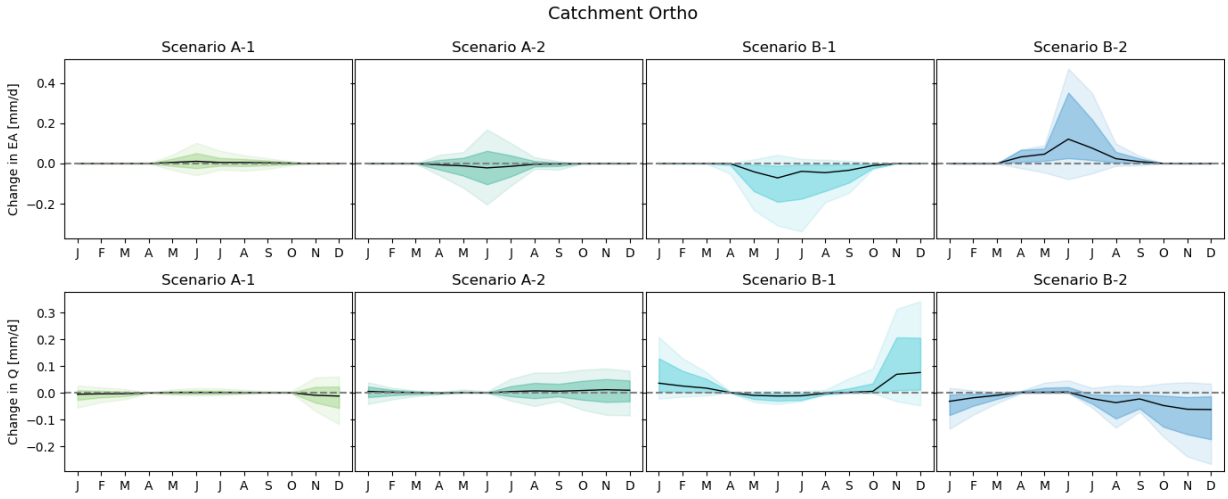

Figure S28: Change in evaporation (EA) and streamflow (Q), both in [mm/d] for Ortho.

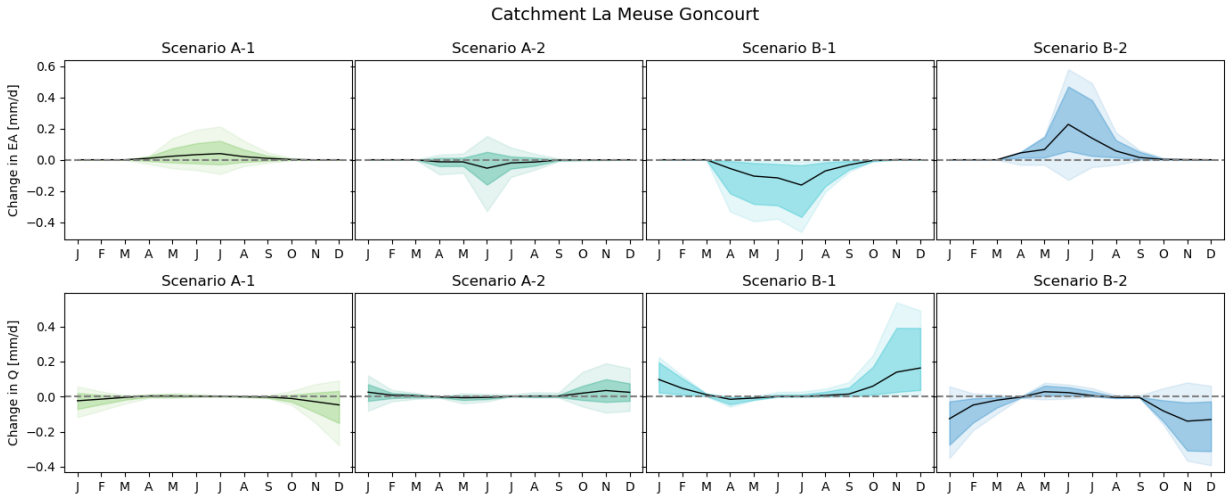

Figure S29: Change in evaporation (EA) and streamflow (Q), both in [mm/d] for La Meuse Goncourt.

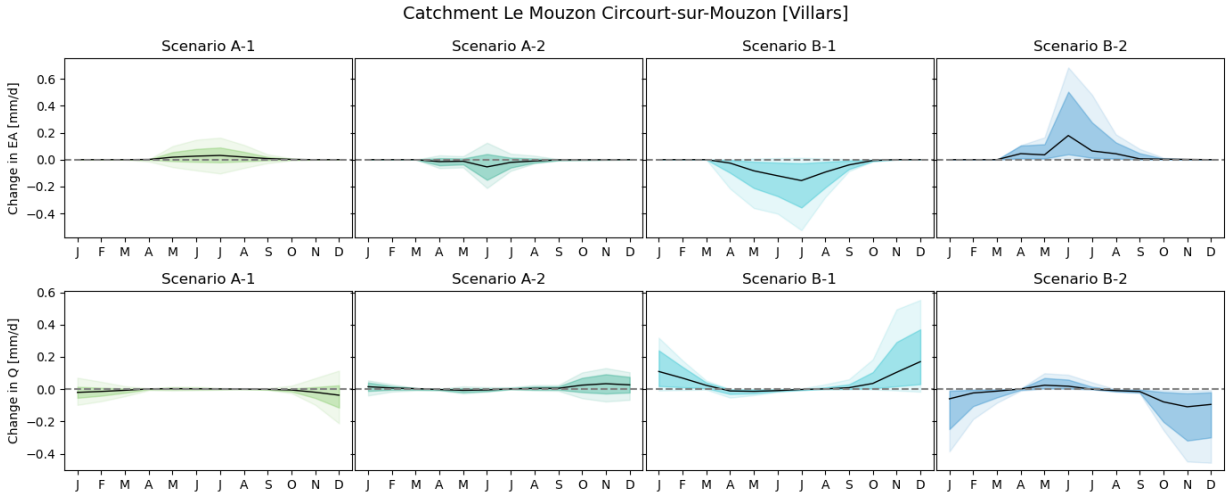

Figure S30: Change in evaporation (EA) and streamflow (Q), both in [mm/d] for La Mouzon Circourt-sur-Mouzon [Villars].

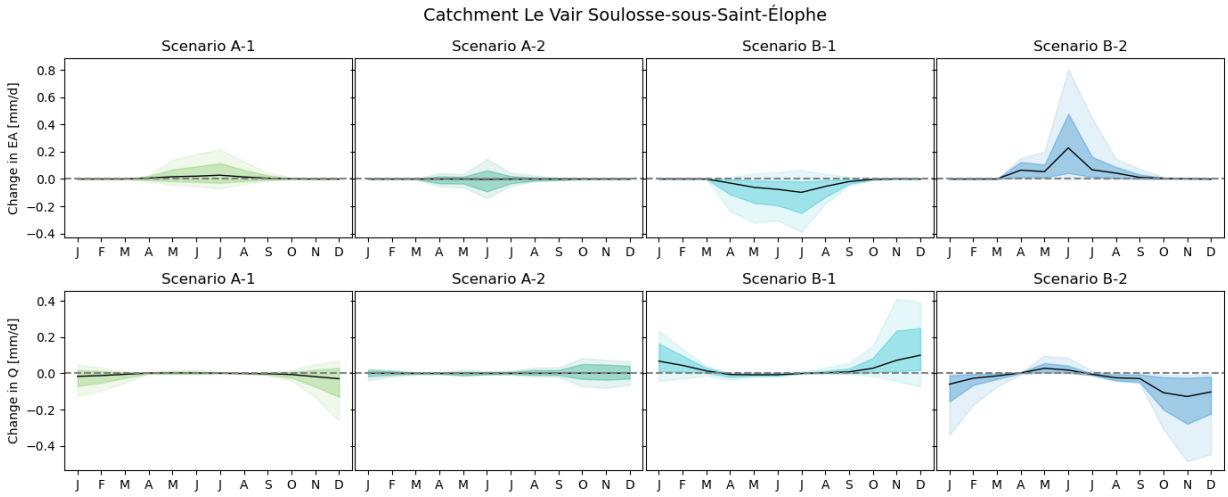

Figure S31: Change in evaporation (EA) and streamflow (Q), both in [mm/d] for Le Vair Soulosse-sous-Saint-Élophe.

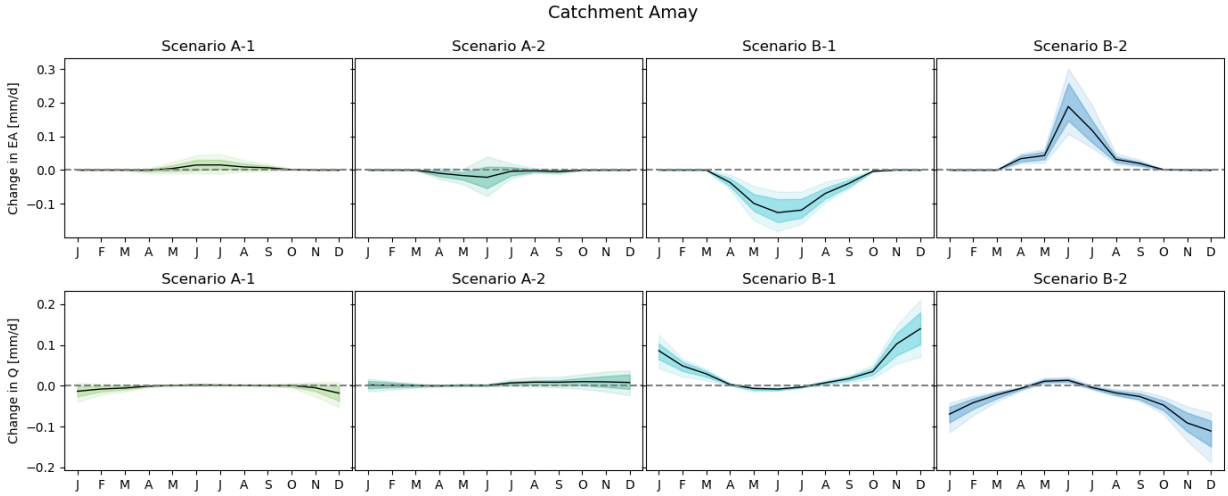

Figure S32: Change in evaporation (EA) and streamflow (Q), both in [mm/d] for Amay.

S7. Change in $Q_{\max}$ and $Q_{\min}$ per catchment

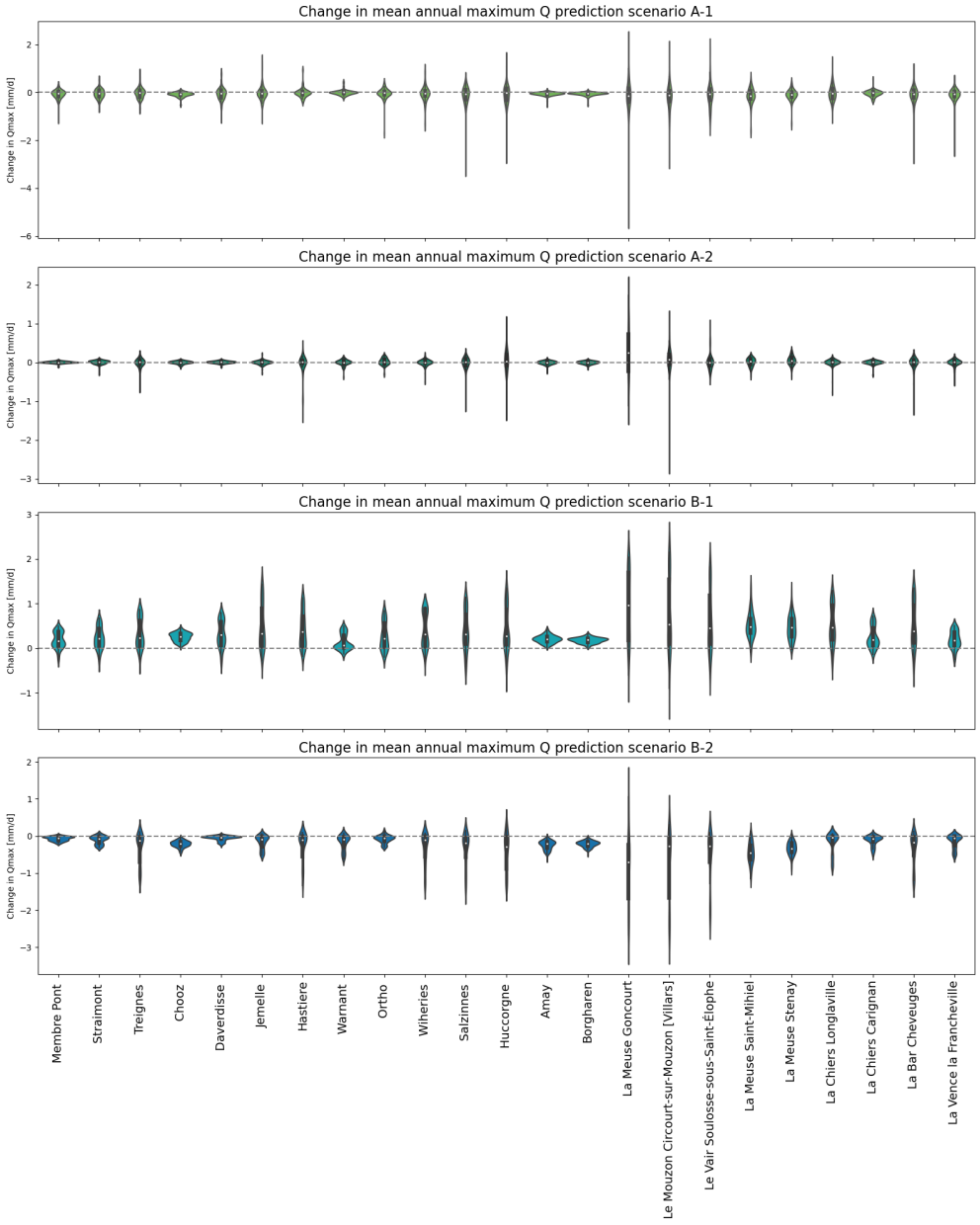

Figure S33: Change in maximum flow ($Q_{\max}$) for each catchment, compared to the reference run, where $\Delta I_E = 0$.

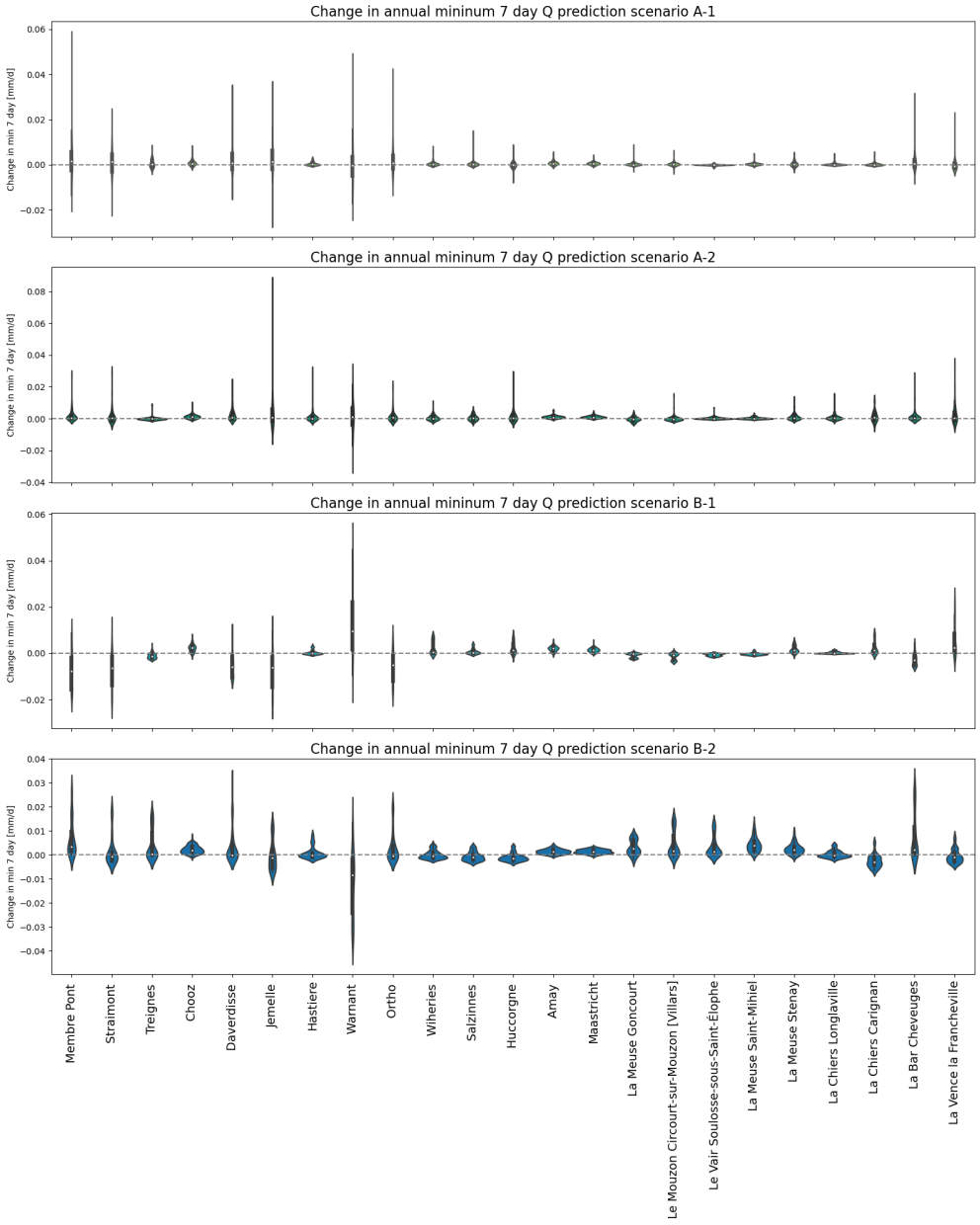

Figure S34: Change in minimum 7 day flow ($Q_{\min}$) for each catchment, compared to the reference run, where $\Delta I_E = 0$.